Supplementary Information:

Practical Challenges in the Development of Photoelectrochemical Solar Fuels Production

Mark T. Spitler, Miguel A. Modestino, Todd G. Deutsch, Chengxiang X. Xiang, James R. Durrant, Daniel V. Esposito, Sophia Haussener, Stephen Maldonado, Ian D. Sharp, Bruce A. Parkinson, David S. Ginley, Frances A. Houle, Thomas Hannappel, Nathan R. Neale, Daniel G. Nocera and Paul C. McIntyre

S1 An Analytical Facility for the Third Party Verifications of PEC Performance

S1a Constraints of the Facility upon Prototype Designs

There will always be an interactive relationship between the formats of PEC devices and the ability of an analytical facility to evaluate them. Attempts at categorizing PEC device formats have included classifications based on the number of semiconductor junctions, tandem architectures vs. series connections, wired and wireless devices, as well as different families of semiconductors such as silicon, III-V, oxides and others.[1] Although these categories are useful for comparing key performance metrics of different device properties, in order to properly develop an analytical facility for prototypes, it is necessary to develop a classification system based on the physical configuration of the prototype itself as well as on its component device architectures.

To start, the boundary of a PEC device is defined as the region where inputs such as reactants and sunlight enter the prototype and the outputs of products and excess reactants leave the prototype. Inside the boundary, the prototype includes components that satisfy the light absorption, catalysis, mass transport, including ionic transport, product separation, and light management functions.[2] These components can be either physically integrated or decoupled, but they need to serve the common function of generating fuels from sunlight. Some common device morphologies that have been studied include membrane separated architectures with absorber length scales from cms to μms, vapor-fed devices, particle-based devices and solar concentrated devices.[3]A common methodology to assess the performance of these devices is required to properly assess the relative potential of each of them.

In addition to the technical interests of the user in prototype and component performance, there are broader interests of the customers. The evaluation of a PEC solar fuels prototype, for example, can produce data that is of vital importance to an industrial R&D program: the peak efficiency of the device, its performance efficiency rise and fall times in a diurnal cycle, its spectral response, and perhaps information about durability. This type of third-party verification of the status of industrial efforts plays an essential role in corporate or investor decision making on the viability of a particular design or research effort. Academic research laboratories may find this external confirmation to be especially useful in interactions with industry, investors or funding agencies.

In order to test prototypes, general test bed dimensions and specifications will need to be provided by the facility to researchers. Dimensions may range between 1-100 cm^2, inlets and outlets for reactants and products will need to be included in the customer's design, and the range of flow rates for reactants will need to be provided. Prototypes will need to separate gas and liquid products internally. If liquid electrolytes are needed, a mechanism for recirculation should be included in the prototype, or provided by the facility if the requirement is simple enough. If solar concentration is needed at the research prototype stage, optical components will need to be included.

Where components of these various prototype designs are concerned, many customers could be served, but components of the device may require additional assembly work for the facility to handle. Given that these components can originate from many different PEC prototype designs this component-oriented analytical component work presents resource challenges to the facility in this role.

It may be that a standard chassis for a PEC cell will have to be developed by the facility so that it can readily evaluate unique device components within the facility's physical testing constraints. As has been discussed above for component testing in the PV facilities, this function of an analytical facility would serve the research community as contract research for researchers who lack the specialized capabilities of the facility. An instrumental dimension that was not available in the development of PV technology is the analytical capability of the end stations of synchrotron beamlines; exploitation of this cutting edge measurement tool may force some physical separation of component evaluation from the activities of a centralized PEC test facility.[4]

PEC component research is a greater interest than device assembly and analysis. Metrics of interest in component evaluation may include achievable photon-to-fuel efficiencies, stability, faradaic efficiency and architectural requirements for light, charge and mass transport. It is at this component level where "benchmarking" is appropriate, when it can inform component selection for specific devices designed for particular markets.

Academic activity in component testing produces the additional advantage of a body of work in the public domain which fosters interaction at all levels of prototype development. However, any facility will be limited in resources and will have to make choices as to what components it can evaluate: single or integrated photoanode/cathodes, spontaneous or assisted fuel production, electrocatalysts, membranes, or liquid electrolytes. If this work is performed for a fee, with time the customer community will determine which services have the greatest value and what the needs of the standard testing protocols for each of them will be.

It is expected that the testing of the electrode and photoelectrode interfaces would be of greatest interest for the community, given the large number of the research groups with a focus on these interfaces. These may include single semiconductor electrodes or complex multi-layered structures that integrate electrocatalysts. In order to test these components, active areas below 100 cm^2 are likely to be needed. For wireless photoelectrodes, the analytical facility would need to specify the target footprint of the photoactive material. If the photoelectrodes require wiring, the structures provided would need to include standard electrical connection points. To facilitate testing, the analytical facility may need to create a standard design of a chassis for this photoelectrode testing and provide it to the R&D community. There are many requirements of such a photoelectrode. They include the ability to handle a range of dimensions from 1 to 100 cm^2, to separate product with either cation or anion exchange membranes, and to tolerate a broad range of the electrolyte pH. They must be able to operate for a reasonable amount of time to assess device stability, from 10-100 hrs, and standard cathodes/anodes should be provided if needed, which may be Pt/IrO_x for acidic electrolytes or Ni for basic electrolytes. Certainly, collection ports are required to capture gaseous and/or liquid products and must be included in the chassis and it also must be constructed from materials that will not corrode in the test environment and contaminate the electrolyte

S1b Measurement Capabilities of the Facility

It is evident from this discussion that a PEC analytical facility will possess general capabilities that encompass and exceed that of the present PV facilities. It will certainly need to test prototypes and components under actively

changing illumination intensity, spectra, and angles that replicate solar illumination under real conditions. Test beds for solar-H_2 devices will need to include outlet gas ports that connect with flowmeters and a gas chromatography system. A minimum gas production higher than the internal device volume, perhaps a hundredfold, will be needed to accurately measure production at pseudo-steady state conditions. Testing solar CO_2 reduction devices will require gas and liquid ports that connect through flowmeters to gas chromatography and liquid chromatography systems. Similar minimum production volumes for detection will apply to these devices.

Studies and surveys have been made of the analytical techniques found by the PEC solar fuels community to be necessary for progress.[5-10] In grouping these needs as either component analysis or device performance analysis, it is evident that the former are more mature in their development since there is no third-party dedicated facility for the latter. With the present PV analytical facilities serving as an example, the measurement capability of a PEC facility will include the most significant of both.

An assessment of this literature[5-10] on the needs of device performance evaluation under illumination reveals a great many experimental techniques, but a list of those with greatest significance will include:

1. Solar-to-fuel efficiency: Maximum instantaneous (equivalent to a PV peak efficiency) efficiency and a time-averaged efficiency, reported both daily (perhaps for the equinox and solstice dates) and annually.

2. Degradation rate: A time-dependent loss in performance, perhaps in μg H_2/h, similar to PEM electrolyzers where it is reported as μV/h.

3. Spectral response: Wavelength-dependent photon-to-current efficiency without an external bias.

4. Faradaic efficiency: The percentage of current passing through the device in the electrochemical pathway of interest, particularly important for CO_2 reduction reactions where many product species are possible.

Among the most informative and useful methods for component characterization under illumination will be:

1. Photocathode/Photoanode J-V validation: Evaluate photocurrent onset potential (V_{oc}) and light-limited current density for photoabsorbers in a half-cell configuration.

2. Degradation rate: A diagnostic durability measurement that reports photocurrent loss, at a fixed potential, vs time. This result can be used to compare between similarly tested components but should not be extrapolated to predict durability of a full device.

3. Spectral response of half-cell absorbers: Wavelength-dependent photon-to-current efficiency at reverse bias.

Many dark analyses of components can be significant and can complement this list of methods, the JCAP dark catalyst benchmarking technique being a prime example.[11]

S1c Artifacts and Attributes in Prototype Evaluation

As experience with PV evaluation has shown, artifacts can occur in the evaluation of device performance. Some attributes of a PEC prototype may amplify the results by design, such as through photon management or product harvesting strategies. These represent real increases in system performance through engineering design, but they can be misleading if absolute values for catalyst efficiency or fuel production under standard conditions are desired. One must be able to distinguish artifacts and isolate their effects; this is an ongoing learning in the evaluation of the performance of solar based devices.

Given the history of prior foundational work on PEC performance, there is already an experience base on revealing artifacts in PEC devices. There are articles and book chapters[13-15] documenting standard measurements which have identified numbers of possible artifacts in PEC fuels production. Common PEC measurements at the device level include J-V sweeps, un-assisted photocurrent measurements, IPCE measurements and direct measurements of hydrogen and/or oxygen generation rates. Common artifacts in PEC measurements can arise from the use of different illumination sources such as tungsten-halogen lamps, xenon arc lamps, or natural sunlight, with or without diffusive light paths, as well as the intensity calibration of the light source stemming from the types of photodiode for light calibration and the placement of the calibration photodiode, both in the distance from the light source as well as in a dry, electrolyte-free location. There can be problems with the definition of the electrode/device area owing to encapsulation methods or the presence of an aperture and there can be effects of the electrolyte absorption and parasitic reactions instead of water-splitting reaction resulting from chemical corrosion and the oxidation/reduction of sacrificial species. Also important are bubble effects on light management, catalytic activity and interfacial stability. There are ongoing efforts in this area to assemble and disseminate information on the definition of best practices in design and analysis, of gaps in knowledge or experience, and of priorities in research on these evaluations.

References:

1. J.W. Ager, M. R. Shaner, K. A. Walczak, I. D.Sharp, S. Ardo, *Energy & Environ. Sci.,* 2015**, 8**, 2811-2824.
2. M. A. Modestino and S. Haussener, *Annu. Rev. Chem. Biomol. Eng.,* 2015, **6**, 13-34.
3. C. Xiang, A. Z. Weber, S. Ardo, A. Berger, Y. Chen, R. Coridan, et al., *Angewandte Chemie Int. Ed.* 2016, **55**, 12974-12988.
4. J. Yano, J. A. Haber, J. M. Gregoire, D. Friebel, A. Nilsson and F. Houle, JCAP Research on Solar Fuel Production at Light Sources, *Synchrotron Radiation News*, 2014, **27**, 14-6.
5. *Photoelectrochemical Water Splitting: Standards, Experimental Methods, and Protocols*, eds: Z. Chen, H. N. Dinh, E. Miller, New York: Springer, 2013.
6. R. E. Rocheleau, E. L. Miller, *Int. J. Hydrogen Energ*., 1997, **22**, 771-782.
7. R. H. Coridan, A. C. Nielander, S. A. Francis, M. T. McDowell, V. Dix, S. M. Chatman, and N. S. Lewis, *Energy Environ. Sci.*, 2015, **8**, 2886-2901.
8. A. B. Murphy, P. R. F. Barnes, L. K. Randeniya, I. C. Plumb, I. E. Grey, M. D. Horne, J. A. Glasscock, *Int. J. of Hydrogen Energ.,* 2006, **31**, 1999–2017.
9. S. Hu, C. Xiang, S. Haussener, A. D. Berger, and N. S. Lewis, *Energy Environ. Sci.*, 2013, **6**, 2984–2993.
10. H. Döscher, J. F. Geisz, T. G. Deutsch and J. A. Turner *Energy Environ. Sci.*, 2014, **7**, 2951–2956.

11. C. C. L. McCrory, S. Jung, I. M. Ferrer, S. M. Chatman, J. C. Peters, J. C. and T. F. Jaramillo, *J. Am. Chem. Soc.*, 2015, **137**, 4347-4357.
12. *Photovoltaic Calibrations at the National Renewable Energy Laboratory and Uncertainty Analysis Following the ISO 17025 Guidelines,* K. Emery, www.nrel.gov/docs/fy17osti/66873.
13. J. L. Young, M. A. Steiner, H. Döscher, R. M. France, J. A. Turner, and T. G. Deutsch, *Nature Energy* 2017, **2**, 17028.
14. H. Döscher, J. L. Young, J. F. Geisz, J. A. Turner, and T. G. Deutsch, *Energy and Environ. Sci.*, 2016, **9**, 74-80.
15. Z. Chen, T.F. Jaramillo, T.G. Deutsch, A. Kleiman-Shwarsctein, A. J. Forman, N. Gaillard, et al., *J. Mater. Res*. 2011, **25**, 3-16.

S2 Challenges in System Prototyping

S2a Configurations of Device Designs

The overview in Fig. 2 in the text of the main classes of schemes and designs for devices for the transduction of solar photons to fuels provides a context for following analyses of PEC prototype design and will aid in the identification of the procedures and techniques for performance evaluation of devices and of components. In any of these designs in Fig. 2, visible light-absorbing semiconductors have long been sought that can serve as effective catalytic interfaces for the redox reactions water splitting, but without success. In response, research has pursued the development of surface deposited inorganic electrocatalysts and molecular catalysts, particularly for water oxidation and extensive benchmarking of HER co-catalysts has been done. [1] Progress has been made and this effort has been extended to electrochemical reduction of CO_2 to useful hydrocarbon compounds, which in liquid form could greatly impact system design and costs.[2]

S2b Frameworks for Decision Trees and PEC Prototype Design

This discussion will focus on photoelectrode-based PECs for hydrogen production from water electrolysis and to a lesser extent fuels derived from CO_2 electrolysis. Particular attention will be given to the task of identifying the electrolyte, where the advantages and disadvantages of each electrolyte type will be highlighted. This selection of an electrolyte as well as the corresponding compatible materials for the cell and device sets the stage for application of electrochemical engineering principles in a follow-up analysis of the prototype scale up. Several distinct types of electrolytes will be reviewed that have been explored to date, as will the implications of their selection for prototype design.[3] In the electrolyzer and fuel cell communities, different types of devices are commonly categorized based on the type of electrolyte that is used, and it is reasonable that this sort of electrolyte-centric taxonomy can be similarly useful for PEC systems. The types of electrolytes used for photosynthetic, fuel-forming PEC devices include aqueous alkaline, aqueous acid, aqueous salt solutions, solid electrolytes, and mixed aqueous/nonaqueous electrolytes. The following discussion highlights key advantages, disadvantages and challenges of each, as well as relevant prototype examples based on these electrolytes.

Aqueous alkaline electrolytes such as KOH or NaOH are fairly conductive at high concentrations, reducing resistance losses in the cell.[4] In this pH region, several earth-abundant electrocatalysts are known that are stable and have fairly low kinetic overpotential losses for OER /HER. Stainless steel and some plastics may be used for balance of systems (BOS) components. There is also an increased number of options for CO_2 electrolysis. In addition, there is much art that be carried over from low-temperature alkaline electrolyzer technology. Of course, a highly caustic electrolyte that requires additional safety considerations, but more significant are the constraints that this pH imposes upon the selection of the semiconductors exposed to solution through exclusion of silicon, some carbides, and WO_3.

Aqueous acids can provide high conductivity through their highly mobile protons and allow facile HER kinetics at the interface, including for some non-precious metals.[1] Although acids are compatible with silicon**,** they are corrosive for many photoelectrode/co-catalyst/BOS compositions that might otherwise be considered such as stainless steel. As with basic electrolytes, they have safety concerns. There is also a lack of stable and efficient non-precious metal electrocatalysts for OER and possible side reactions with anions must always be considered.

Aqueous salt electrolytes at a neutral pH such as Na_2CO_3, NaCl, Na_2SO_4, whether buffered or not, are cheap and readily available. This class of electrolytes can enable the use of some electrode solids that are not stable at acidic/alkaline pH, which may be of interest for certain chemistries, such as direct CO_2 electrolysis.[5,6] However, they do have lower conductivity, although at solar luminance the currents are at a low, 30 mA/cm^2 compared to 1 A/cm^2 in commercial electrolyzer units. They must be integrated into a compatible device design where the kinetics of the HER and OER are fast. There are possible side reactions, and large pH gradients will develop unless buffered or compensated by device design. Bipolar membranes would find a useful role in this environment, but less promising outcomes would be expected if coupled with a solid electrolyte membrane.

Solid electrolytes such as Nafion® or an OH^- exchange membrane can enable very small gaps between electrodes while serving as a membrane separator.[7,8] Bipolar membranes can enable operation with two different pH regimes[9] and can operate with an air-fed electrolysis. One can leverage membrane developments from electrolysis and fuel cell fields. Incorporating such crossover membrane components to a PEC design can add cost and potentially design complexity. They can be susceptible to degradation/fouling, can block light, may have low permeability for certain ions, and may allow cross-over at low current densities of many PEC designs.

Mixed electrolytes of aqueous/ionic liquid or mixed aqueous/solid electrolytes may allow enhanced mass transfer and present another control parameter for (photo)electrocatalysis, allowing the inclusion of two efficient PEC solids that may be optimized for different pH environments.[10,11] Such mixed components do increase cost. They may also suffer from settling, interfere with light absorption and suffer from degradation of non-aqueous component.

With this review of the advantages and disadvantages of various electrolyte types of interest for PEC prototypes, the implications of the choice of the electrolyte on prototype/system design become evident through the lens of a decision tree. The particular electrolyte composition determines its conductivity, a key parameter in electrochemical engineering, which in combination with average distance between electrodes, determines what solution iR losses will be incurred at a desired operating current density. Together with kinetic and mass transfer overpotential losses, these ohmic losses determine the minimum photovoltage that must be generated by the illuminated semiconductor at the desired current density, whether it be a single, tandem or multiple junction stack of photoabsorbers. (Here the photovoltage is taken as a measure of the non-simple relation of the velocities of catalytic reactions, electron-hole recombination and production of reactive charge carriers at the semiconductor surface.) Conversely, for a maximum acceptable iR loss, in this way the photovoltage also controls the average spacing between electrodes in a scalable design. Other implications of the choice of electrolyte, combined with the desired product, will include selection of

the location of product formation, whether it be in-device vs. downstream, as has been mentioned in possible CO_2 reduction schemes with H_2, and the mechanism of separation of products from reactants and from each other, as well as the choice of materials of construction for the BOS.

Having established a central role that the choice of the electrolyte type plays in materials selection and prototype design, a hypothetical decision tree is now presented as an example of a high-level framework for selecting materials and prototype architectures. In this example, the flow of the decision tree begins with the discovery of a novel and highly effective semiconductor for photoabsorption. This tree is depicted in Fig. 3 of the text and is repeated here for clarity with the input of the novel solid, integrated with any challenges in its materials processing. The selection of the target fuel as molecular hydrogen or a carbon-based fuel is made at node D1. The choice of fuel, combined with knowledge of the properties of the new semiconductor, leads to decision point D2 in Fig. 3 below when the electrolyte is selected. This decision should be heavily influenced by the known stability properties of the new photoabsorber material, as well as knowledge of the redox chemistry that will be involved with production of the target fuel. Importantly, selection of the electrolyte type will set significant constraints on downstream decisions for the reasons discussed in the previous sections.

If a tandem configuration is selected at D3, the band gap and other optical properties will recommend its use as top or bottom cell and this sets up the architecture at for the prototype at D4. With a decision already being made on electrolyte and desired fuel of interest, what remains is the selection of the appropriate co-catalysts, coatings, and materials for the D5 balance of system decisions. This hypothetical decision tree concludes with the identification of a tandem system with a louvered configuration, as shown in Fig.2-1 as one of several options, operating in aqueous alkaline electrolyte with NiOOH/Ni catalytic surface layers. This particular example illustrates the use of a decision tree for a basic researcher. It should be noted that for an industrial concern that has already identified its market size and BOS advantages, points D4 and D5 may well be fixed at the beginning of the process.

It is clear from this example that there are challenges as well as opportunities for the improvement and use of such design frameworks for the development of PEC prototypes. Establishing a select number of decision trees as guides for some of these commonly encountered design problems could be of great value. The decision tree shown in Fig. 3 below displays one possible series of decisions associated with the design of a prototype beginning at one specific starting point and is neither exclusive nor unique. For example, the order of key decisions in prototype design might be very different if the starting point were the choice of a target chemical or fuel or the discovery of a new electrocatalyst. It might also be possible to start with the conception of a new PEC device design, progressing down a series of decisions that will determine the materials, operating conditions, and geometric characteristics for an optimized prototype system.

Materials informatics tools and databases might help automate the generation of options and decision making through an online platform. This would have to be integrated with the means to add research learning to these databases.

Although this hypothetical design platform is not yet a reality, many of the individual tools required to make it real already exist or are maturing quickly. When mature, AI approaches may prove valuable in this role.

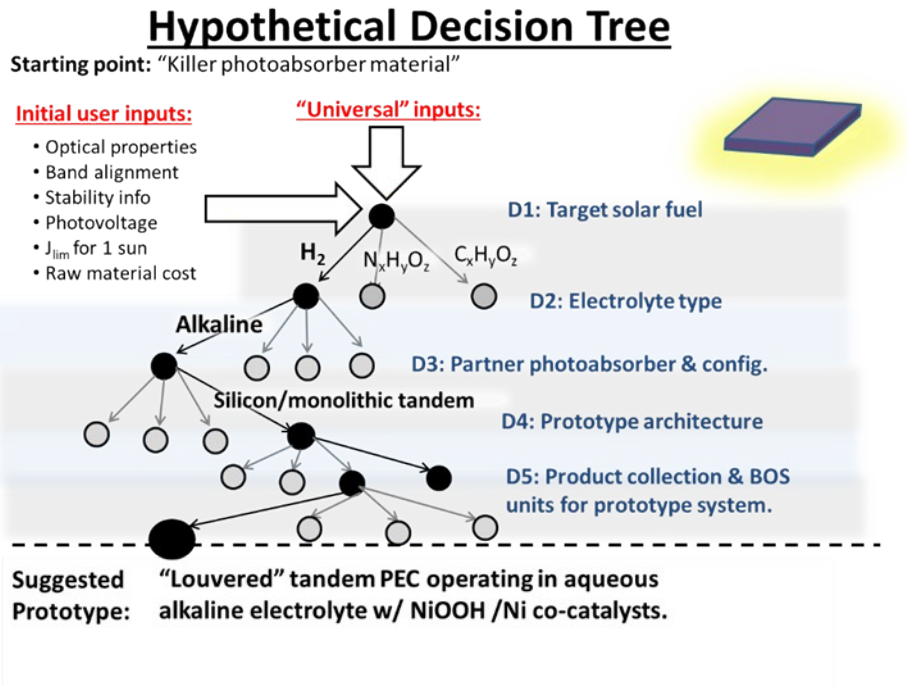

Fig. 3 (from text) An example of a Decision Tree for the design of a PEC device for solar fuels production that starts its flow with a novel photoabsorbing semiconductor and concludes with a prototype design. Details on the use of this Decision Tree are given in **S2**.

S2c Device Scale-up and System Operation under Realistic Conditions

There are a number of unique characteristics in PEC systems and devices that are not present in technologies related to PEC. Electrochemistry is not to be found in solid state PV nor are light absorption and semiconductor physics in electrolyzer technologies, for example. However, this aspect of PEC cells does allow the broader range of multi-dimensional or anisotropic design approaches such as those shown in Fig. S2-1 with louvers, side-by-side cells, or micro-wire designs with orthogonalization of transport. Another challenge which is present in any solar-driven PEC process is the low energy density of a typical yearly-average of ~300 W/m^2, which requires large collection areas. While it is clear that for PV applications outside of concentrated solar power the radiation collection area equals to the PV cell area, this is not necessarily the case for PEC devices. For a monolithic device design with separate photocatalysts for both oxidation and reduction as shown in Fig. S2-1, then yes. However, if a photoabsorber or photocatalytic surface is used that employs an additional dark co-catalyst on the counter electrode, then only the

photoactive part has to equal the collection area. This provides an additional design flexibility, exemplified by the current dilution factor[13,14] or generally co-catalyst application with specific patterns.

However, for PEC devices the low energy density of the solar radiation may have a favorable impact on the reactant requirements. It may be that the water vapor in the air might be sufficient to provide enough reactant to satisfy the need.[15] Consequently, liquid water fed systems might not be required or might allow a concentration of the energy carrier made upstream of the catalytic step by either concentrated solar irradiation or charge carrier concentration. An appropriate matching of the energy and mass fluxes might be a very first step of a PEC device design.

An examination of scale-up losses and their origins is possible in the case where performance is the main driver in the device design and this can be done initially with the aid of simple 0D models or equivalent circuit modeling. In this process, quantitative and qualitative information can be generated, defining the required series and shunt resistance in the photoabsorber and ohmic losses in the electrolyte as well as all solid conductors. The latter are usually negligible in lab-scale devices unless high current density operation is targeted, for example, through high irradiation concentration. Activation overpotentials can be estimated based on the calculated current density vector field distribution in the catalytically active sites. Concentration overpotentials can be estimated based on the calculated concentration fields in PEC devices operated in batch or continuous flow.

The complicated and coupled multi-physics nature of functional PEC devices and scale-up activities points to the general need for modeling frameworks and the relevant experimentation which can deconvolve the influence of materials, operating conditions, and design on the device performance. The scale-up of a prototype from laboratory scale to a manufacturing prototype commonly requires a “re-invention” of the device since seemingly irrelevant materials in the substrates or chassis or processes for the deposition usually have to be modified or replaced. What becomes apparent in multi-dimensional device simulations and experimentation in scale up are the particular non-uniform current densities, temperatures, and species concentrations throughout the device that are generally enhanced by increasing sizes. Only multi-dimensional models have the potential to be used in the assessment of the impact of this aspect of scale-up. Opportunities for new designs may be created through such modeling. Insight can be gained not only on the optimum size of the scaled device but also the relative sizes of the auxiliary components, such as pumps. Here, insights and benefits can also be gained by a careful review of other technologies.

The discussion of device performance and modeling is usually based on a steady state investigation, where a device is optimized for a given design point. It is clear that the power and load curve of a real PEC device will drift with time, especially with respect to the spectrum and intensity of irradiation, arguing for an optimization based on an expectation of a dynamic operation.[16,17] The ability to characterize these dynamics must be developed for PEC devices so that their effect upon design can be established and the determination of the representative design point can be made.

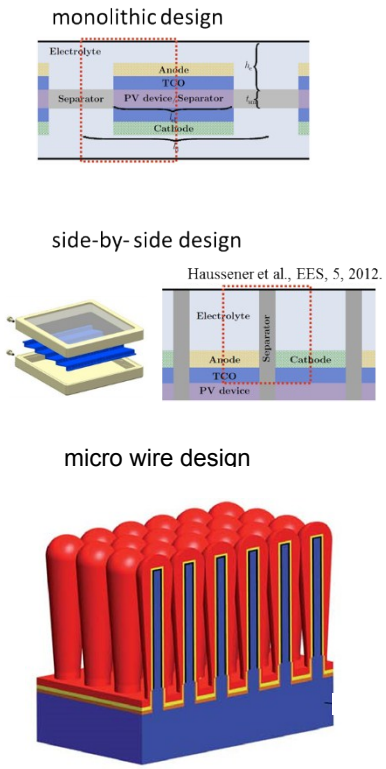

Fig. S2-1 (a) The versatility of design inherent in a PEC solar fuels device is depicted in a monolithic as well as a side-by-side design with louvers (with permission from ref. 26). (b) Micro-wire constructs have also been made where WO_3 has been deposited about a Si nanowire array (with permission from ref. 12).

References:

1. C. C. McCrory, S. Jung, I. M. Ferrer, S. M. Chatman, J. C. Peters, and T. F. Jaramillo, *J. Am. Chem. Soc.*, 2015, **137**, 4347-4357.
2. A. Singh, J. Montoya, J. Gregoire, and K. Persson, *Nat. Comm.*, 2019, **10**, 443.
3. J. Turner, *Nat. Mater.*, 2008, 7, 770-771.
4. B. A. Pinaud, J. D. Benck, L. C. Seitz, A. J. Forman, Z. Chen, T. G. Deutsch, et al., *Energy Environ. Sci.*, 2013, **6**, 1983-2002.
5. Y. Tachibana, L. Vayssieres and J. R. Durrant, *Nat. Phot.*, **6**, 511–518.
6. M. A. Modestino, K. A. Walczak, A. Berger, C. M. Evans, S. Haussener, C. Koval, et al., *Energy Environ. Sci.*, 2014, **7**, 297-301.
7. T. Bosserez, L. Geerts, J. Rongé, F. Ceyssens, S. Haussener, R. Puers and J. A. Martens, *J. Phys. Chem. C*, 2016, **120**, 21242-21247.
8. W. White, C. D. Sanborn, D. M. Fabian, S. Ardo, *Joule*, **2**, 2018, 94-109.
9. K. Sun, R. Liu, Y. Chen, E. Verlage, N. S. Lewis and C. Xiang, *Adv. Ener. Mater.*, 2016, **6**, 1600379.
10. M. B. McDonald, S. Ardo, N. S. Lewis and M. S. Freund, *ChemSusChem*. 2014, 7, 3021-7.
11. S. Y. Tembhurne; F. I. Nandjou Dongmeza and S. Haussener *Nature Energy*, 2019-04-29.

12. M. R. Shaner, K. T. Fountaine, S. Ardo, R. H. Coridan, H. A. Atwater and N. S. Lewis, *Energy Environ. Sci.*, 2014, **7**, 779-790.
13. C. A. Rodriguez, M. A. Modestino, D. Psaltis and C. Moser, *Energy Environ. Sci.*, 2014, **7**, 3828-3835.
14. M. Dumortier and S. Haussener, *Energy Environ. Sci.*, 2015, **8**, 3069-3082.
15. T. A. Kistler, D. Larson, K. Walczak, P. Agbo, I. D. Sharp, A. Z. Weber and N. Danilovic, *J. Electrochem. Soc.*, 2019, **166,** H3020.
16. S. Haussener, S. Hu, C. X. Xiang; A. Z. Weber; N. S. Lewis*, Energy Environ. Sci.,* 2013, **6**, 3605-3618.
17. S. Tembhurne and S. Haussener, *Sustainable Energy Fuels*, 2019, **3**, 1297-1306.

S3 Novel Semiconductors and Coatings

S3a Exploration of a Materials Class - Adamantine Semiconductors

In this discussion on the discovery of new semiconducting solids, it is useful to examine a known class of adamantine semiconductors depicted in Fig. S3-1, as an example of how to exploit, optimize and utilize a class of solids once they are discovered.[1] As indicated above, this particular class of compounds may be too expensive to employ in a practical device, but their examination does allow the development of critical analysis, thinking and methods development during the period when other, more suitable solids are being discovered and developed. This discussion highlights the many possible variations within a class of photoactive solids that present many opportunities for use in a PEC application.

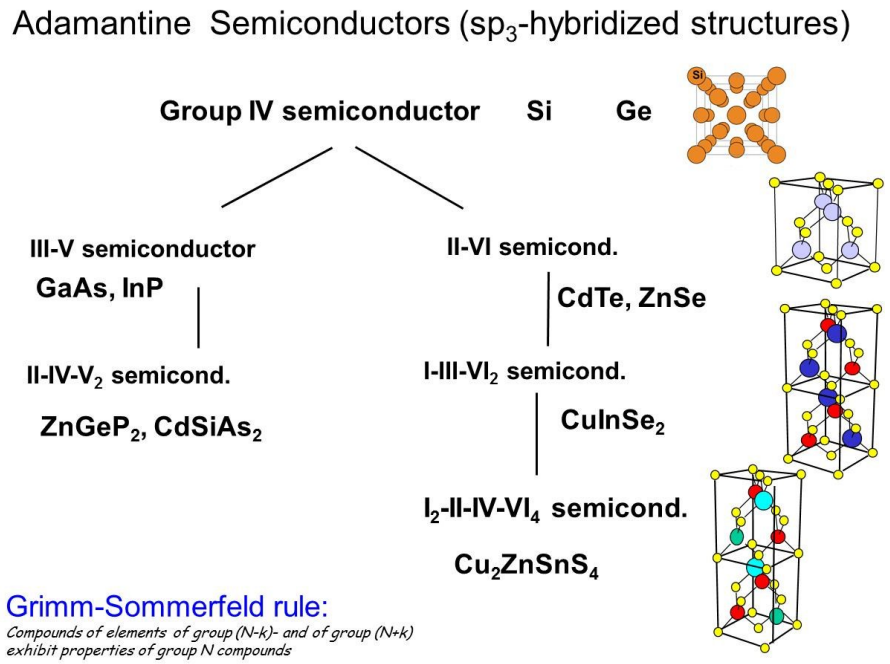

Fig. S3-1 The adamantine semiconductors under discussion are depicted in an arrangement centered on the Group IV semiconductors Si and Ge and in varying composition with elements from neighboring columns on the periodic table.

The attraction of the adamantine semiconductor material class for a wide range of electro-optical applications is that their electronic structure may be tuned smoothly via the composition of multinary compounds.[2] The tunability of the bandgap over wide ranges of the solar spectrum can enable high-efficiency energy conversion. For a dual absorber tandem structure, the optimum photovoltaic efficiencies of the two component cells would require band gaps of

around 1.1 eV and 1.7 eV; the combination of III-V semiconductors and Si here promises efficiencies close to optimum. Such a tandem absorber device requires ideal preparation of all of the many interfaces involved[3-4] with a control and understanding of the interface formation step by step. Low non-radiative recombination rates in the bulk as well as at the interfaces are essential for these applications. The solids are available as wafers, which facilitates the preparation of smooth and high-quality reference surfaces on homoepitaxially grown buffer layers. Chalcopyrite and kesterite compounds are also tunable with regard to the electronic structure and lattice constants, but within a more limited range of parameters, in particular, in the important region of higher energy gaps greater than 1.5 eV.

The efficient multi-junction devices in PV technology provide a model for the insertion of novel tandem designs into PEC solar fuel devices. In PV the crucial characteristics for feasibility are efficiency and stability. Conversion efficiencies benefit greatly with the use of multi-junction absorbers to increase the use of the solar spectrum and generate enough photovoltage to drive the reactions. In monolithic multi-junction solar cells, multiple single junction solar cells with different band gaps can be connected in series. The subcells are selected with appropriate band gaps in an efficient generation of photovoltage and photocurrent in portions of the solar spectrum to ensure the current-matching of the different subcells. To facilitate photocurrent flow, a number of tunnel junctions of low-resistivity materials are inserted between each adjacent semiconductor cell surrounded by charge separating contacts in order to control the direction of photocurrent in the device. [5] Logically, such considerations need not limited to solar hydrogen production alone and should extend in great part to other solar fuel approaches, such as CO_2 reduction.

III–V materials are highly tunable in their bandgaps, band offsets and lattice-constants through the choice of the stoichiometry of multinary compounds. Their deposition through organic vapor phase epitaxy (MOVPE) is well-established for at an industrially relevant scale, with significant progress having been made in the field of III–V-on-Si heteroepitaxy by MOVPE and subsequent III–V nucleation with major advances in *in situ* process control and *ex situ* analysis.[6] Density functional theory (DFT) and kinetic growth simulations continue to explain details of the formation of critical surfaces, nucleation, interfacial reactions and film growth in complex environments such as ambient vapor phase.[7]

Size-tunable quantum structures such as quantum wells or nano wires can also be employed with this class of semiconductor materials. The separated electronic states of electrons and holes in these structures offer opportunities to accumulate charge carriers in well-defined states. In such structures, possible benefits can be realized in an increased absorption coefficient and slower electron relaxation through phonon-bottlenecks.[8] The energetics and dynamics of excited electronic states, charge transport and charge separation could be fine-tuned to the specific needs of the envisaged device. It has been shown that quantum well structures can be controlled via strain-balancing to provide means to adjust the absorption edges. In planar multiple quantum well structures, however, charge carriers have to pass multiple times through the different quantum wells which increases the probability of capture and of non-radiative recombination. This is avoided in axial and radial III-V nanowire structures which have been grown with a catalysis-assisted vapor-liquid-solid growth method in a bottom-up approach.[9] If photostability were to be built into the structure, the result would be a photovoltaic concept opening opportunities and advantages owing to

a greatly increased surface area, a much smaller interface area between nanowires and substrate, and a design featuring much shorter charge transfer distances.

S3b Combinatorial Discovery and the Coupling of Computational and Experimental Materials Science

Given the opportunities presented by the oxides and the fact that no other semiconductors have emerged that have proven to be efficient, stable and inexpensive, a number of groups focused on this class of materials have employed combinatorial techniques to produce and screen libraries of compounds for their water splitting activity.[10-15,17] Challenges for oxide semiconductors include tolerance of acid and a charge transport rate not compromised by polaron formation. The combinatorial approaches for producing metal oxide libraries include, ink jet printing,[11] sputter deposition,[12,14] spray pyrolysis and pulsed laser deposition[10] and in some cases including theoretical calculations to guide the library selection.[13] These efforts on oxides have identified and studied several promising elemental combinations,[16] but progress is in its early stages.[15,17]

It should not be expected that electrocatalysts for H_2 and O_2 evolution should work well on bare semiconductor substrates. So once a promising absorber material is identified, a combinatorial strategy of variation of composition and coverage of catalysts on the absorber surface is expected in the optimization of PEC efficiency and durability.

S3c Coupling Computational and Experimental Materials Science

Empirical, laboratory-based synthetic quests for new PEC materials and electrolysis materials will be inherently slower than computational explorations.[18] A good example of computational capabilities is the ability to look more broadly at the polymorphic family for a particular stoichiometry.[19]

TiO_2 is well known in this respect and shows diverse properties for anatase, rutile and brookite, all of which are potentially PEC materials. It has become feasible to target a structure based on its functionality where that could be light absorption and carrier transport, catalytic ability or stability. Polymorphic diversity is observed broadly, as is shown in Fig. S3-2 for various metal oxides. In many of these families and for chalcogenides and nitrides, for example, there is a broad range of possible polymorphs that could be accessed with appropriate synthetic means. This diversity increases with multinary materials and opens a broad and little explored area for electrochemistry in general and PEC in particular. Good examples include brookite TiO_2 and bernessite/hausmanite MnO_2[19-21] which are good OER catalysts. In addition to the simple crystalline materials it has been shown recently that systems such as ZnO-MnO can stabilize new polymorphs or amorphous materials with potentially superior PEC properties.[22]

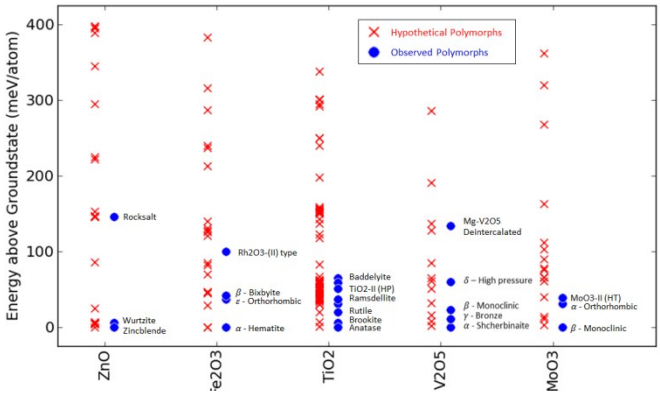

Fig. S3-2, Polymorphic diversity for some well-known systems; red are computationally identified and blue are synthesized. (From ref. 19 with permission. Copyright 2016 Science).)

While the computational tools to predict new PEC materials have improved dramatically, making the compounds is another manner. To this end recent efforts in computational materials science have begun to address the ability to predict synthetic pathways with some notable successes.[18] While this remains an exercise focused on thermodynamics there is hope in the next couple years of being able to better address kinetics and interfaces. However, there has already been some significant progress for solution-based approaches where Pourbaix diagrams can be calculated; substrate matching for targeting a particular polymorph can be accomplished now with the inclusion of strain energies. The latter has worked particularly well for the identification of a substrate to grow the 4mm structure for strontium hafnate which was predicted and realized to be piezoelectric. Finally, by considering critical factors for the evolution of structure types in the growth of MnO_2 and related polymorphs by hydrothermal or solution approaches, it has been possible to target particular ranges where the synthesis of a known or unknown polymorph could be achieved.[20] Some of the key factors are nucleation diameter, pH and associated ion concentrations in solution.

Overall, the ability to identify potentially interesting structures and their functionality, when coupled with some insight on how to achieve them synthetically, may open a significant new window into the development of new materials for PEC. The optimization of a new semiconductor or semiconductor stack can therefore be done first by combining chosen polymorphs, alloys and amorphous materials *in silico*. Weak links in the computational framework do exist and need to be identified and better theory needs to be developed, especially for hybrid materials and for interfaces, both buried and at the surface. Dynamics also present a challenge, but if both kinetics and interfaces could be addressed, this would enable a significant advance in the field of PEC and electrochemistry in general. Finally, many of the techniques being modeled are scalable – i.e. their synthetic methods can be suitable for roll to roll processing. So if the synthesis can be defined to make large area materials uniformly, this could enable the long sought transition to large area for PEC.

S3d Chemical challenges for large area processing of high performance materials

There is a significant base of experience in large area materials deposition which spans a range of wet and dry deposition technologies.[23] An initial approach to new chemistries for thin film synthesis and deposition is to take advantage of controlled chemical and physical interactions at all stages of the film growth process, with selection of reactants and conditions appropriate to continuous processing. The idea is to fully synthesize the desired material on-the-fly rather than rely on post-processing to create it. Post-processing can involve baking or annealing in a controlled atmosphere within a temperature range that avoids degradation. It can fine-tune some aspects of film structure and composition, but not correct the overall elemental balance and spatial arrangement that determines its performance.

The key properties of thin film-substrate systems include their electronic and optical characteristics, mechanical stability, chemical stability during processing, and optimized interfaces. At the atomic level, this means that nucleation and growth of multi-element films on the base substrate or another film must provide the precise stoichiometry required. The chemical kinetics involved require that the rate of formation of nuclei and their accretion be balanced in order to achieve the desired grain size and texture as well as the elemental stoichiometry. This balance may vary through the film thickness in order to provide optimum interfaces on a time frame compatible with the residence time of the substrate in the deposition reaction zone. There are three major variables to consider.[24-30] the chemical nature of the substrate surface, the chemical precursors used and their formulation if application is under wet conditions, and temperature. Each of the three needs to be optimized for the substrate residence time in the processing region and the desired final film thickness. Preparation of the surface to control wetting and nucleation site density will provide control over film uniformity and texture. A crucial step is the selection of specific precursors to control molecule-substrate interactions and the rates of unimolecular and bimolecular reactions relative to surface diffusion and solvent evaporation; it may be that the optimum precursors for the initial stage of growth are different from those to be used for the main film bulk. Programmed temperature variations using a combination of overall temperature and application of flash heating at specific times offer control in a similar way over relative rates of the activated processes that occur. It may be that a fluid environment leads to superior materials relative to one in which the solvent evaporates too fast or molecules decompose too quickly, for example, and temperature vs time control can allow the relative rates to be optimized. Chemical processes for multilayered structures must be selected to control the specific interfacial chemistry and interface width, and these may differ from bulk growth processes.

While each aspect of the chemistry for these materials can be designed and understood in stages, putting them all together into a well-controlled and reproducible process for synthesis will require the concurrent development of accurate and predictive chemical models.

References:

1. C. S. Schnor, *Appl. Phys. Rev.*, 2015, **2**, 031304.
2. S.-H. Wei and A. Zunger, *J. Appl. Phys.*, 1995, **78**, 3846.
3. O. Supplie, M. M. May, S. Brückner, N. Brezhneva, T. Hannappel and E. V. Skorb, *Adv. Mater. Int.* 2017, **4,** 1601118.
4. M. M. May, H.-J. Lewerenz, D. Lackner, F. Dimroth and T. Hannappel, *Nat. Comm., 2015,* **6**, 8286.
5. M. M. May, D. Lackner, J. Ohlmann, F. Dimroth, R. van de Krol, T. Hannappel and K. Schwarzburg, *Sustainable Energy Fuels*, 2017, **1**, 492-503.
6. H. Doescher, GaP Heteroepitaxy on Si(100), PhD Thesis, Technical University, Ilmenau, 2013.
7. O. Romanyuk, O. Supplie, T. Susi, M. M. May and T. Hannappel, *Physical Review B*, 2016, **94**, 155309.
8. A. J. Nozik, M. C. Beard, J. M. Luther, M. Law, R. J. Ellingson| and J. C. Johnson *Chem. Rev.*,2010, **110**, 6873–6890.
9. B. M. Kayes, M. A. Filler, M. C. Putnam, M. D. Kelzenberg, N. S. Lewis and H. A. Atwater, *Appl. Phys. Lett.*, 2007, **91**, 103110.
10. K. Majhi, L. Bertoluzzi, , K. J. Rietwyk, , A. Ginsburg, D. A. Keller, P. Lopez-Varo, et al., *Adv. Mater. Interfaces*, 2015, **3**, 1500405–8.
11. P. N. Anunson, G. R. Winkler, J. R. Winkler, B. A. Parkinson, B. A. and J. D. Schuttlefield Christus, *J. Chem. Ed.*, 2013, **90**, 1333–1340.
12. K. Sliozberg, H. S. Stein, C., Khare, B. A. Parkinson, A. Ludwig and W. Schuhmann, *ACS Appl. Mater. Interfaces*, 2015, **7**, 4883–4889.
13. Q. Yan, J. Yu, S. K. Suram, L. Zhou, A. Shinde, P. F. Newhouse, et al., *PNAS*, 2017, **114**, 3040–3043.
14. L. Zhou, Q. Yan, A. Shinde, D. Guevarra, P. F. Newhouse, N. Becerra-Stasiewicz et al., *Adv. Ener. Materials*, 2015*,* **5**, 1500968–13.
15. J. M. Gregoire, C. Xiang, S. Mitrovic, X. Liu, M. Marcin, , E. W. Cornell, et al., *J. Electrochem. Soc.*, 2013, **160**, F337–F342.
16. C.-M. Jiang, G. Segev, L. H Hess, G. Liu, G. Zaborski, F. M. Toma, et al., *ACS Appl. Mater. Interfaces*, 2018, **10**, 10627-10633.
17. L. Zhou, Lan, A. Shinde, S. Suram, H. Stein, S. Bauers, A. Zakutayev, et al., *ACS Energy Lett.*, 2018, **3**, 2769-2774.
18. K. Alberi et al., *J. Phys. D: Appl. Phys.,* 2019, **52**, 013001.
19. W. Sun, S. T. Dacek, S. P. Ong, G. Hautier, A. Jain, W. D. Richards, et al., *Sci., Adv.*, 2016, **2**, e1600225.
20. D. A. Kitchaev, S. T. Dacek, W. Sun and G. Ceder, *J. Am. Chem. Soc.*, 2017, **139**, 2672-2681.
21. J. Haggerty, J.Mangum, O. Agirseven, J. D. Perkins, L. Schelhas, D. A. Kitchaev, et al., *J. Non-Cryst. Sol.*, 2019, **505**, 109-114.
22. A. M. Holder, S. Siol, P. F. Ndione, H. Peng, A. M. Deml, B. E. Matthews, et al., *Sci. Adv.,* 2017, **3**, e1700270.
23. US Department of Energy Quadrennial Technology Review 2015, Chapter 6: Innovating Clean Energy Technologies in Advanced Manufacturing https://www.energy.gov/quadrennial-technology-review-2015A
24. J. De Yoreo, P. U. P. A. Gilbert, A. J. M N. Sommerdijk, R. L. Penn, S. Whitelam, D. Joester, et al., *Science,* 2015, **349**, 498.
25. S.G. Kwon and T. Hyeon, *Accts. Chem. Res.*, 2001, **48**, 1696-1702.
26. H. Cölfen and S. Mann, *Angew. Chem. Int. Ed.*, 2003, 42, 2350-2365.
27. N.T.K. Thanh, N. Maclean and S. Mahiddine, *Chem. Rev.*, 2014, **114**, 7610-7630.
28. Jai Il Park, Amir Saffari, Sandeep Kumar, Axel Gunther and Eugenia Kumacheva, *Ann. Rev. Mater. Res.*, 2010, **40**, 415-443.
29. J. A. Lim , W. H. Lee , H. S. Lee , J. H. Lee , Y. D. Park and K. Cho, *Adv. Funct. Mater.*, 2008, **18**, 229-234.
30. L. Yu, M. R. Niazi, G. O. Ngongang Ndjawa, R. Li, A. R. Kirmani, R. Munir, A. H. Balawi, F. Laquai and A. Amassian, *Sci. Adv.*, 2017, **3**, e1602462.

S4 Durable Interfaces

S4a Interfacial Kinetics and Failure Mechanisms

Considerations of the fundamental factors relevant to semiconductor corrosion in aqueous electrolytes have shown how the degradation of the semiconductor/electrolyte interface can follow either electrochemical or chemical pathways, or a combination of the two. As developed by Gerischer,[1] the thermodynamic criteria for electrochemical degradation can be understood using the quasi-Fermi level concept. Specifically, if the potentials ascribed to the reductive and oxidative degradation pathways ($_{n}\mathbf{E}_{decomposition}$ and $_{p}\mathbf{E}_{decomposition}$, respectively)

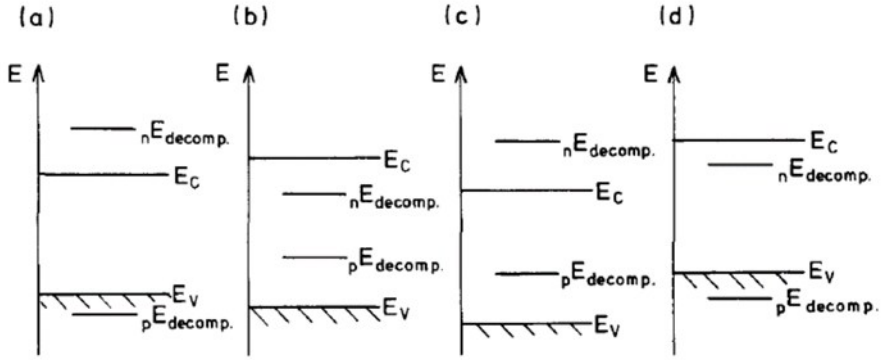

Fig. S4-1. Typical correlations between energy positions of band edges and decomposition potentials that control the thermodynamic stability against photodecomposition. (a) Stable, (b) unstable anodically and cathodically (c) stable against cathodic decomposition, and (d) stable against anodic decomposition. (From Ref. 1 with permission. Copyright 1972 Elsevier.)

fall within the band gap, then the average energies of electrons and/or holes will be able to energetically drive these deleterious redox processes, as is depicted in Fig. S4-1. Conversely, if one or both of the relevant degradation potentials lie outside the bandgap, the material will not undergo electrochemical degradation during operation. A number of estimates of $_{n}\mathbf{E}_{decomposition}$ and $_{p}\mathbf{E}_{decomposition}$ for a variety of semiconductor materials have been made.[2] In this picture most all of the light absorption occurs in the bulk, whereas decomposition occurs at the surface, implying that transport is not a limiting factor, which is not always a safe assumption. Reactive Fe_2O_x PEC electrodes are an example, where hole diffusion lengths of 1-10 nm limit their practical utility.[3]

The thermodynamic nature of the Gerischer model does not speak to the kinetics of the surface reactions. It also does not relate to the susceptibility of a material to chemical degradation reactions which may be active at pH 0 or 14 during surface redox reactions where protons are either consumed or produced locally at the electrode surface,[4] nor does it predict the surface decomposition process, which could result in a stable passivation layer that might enhance the lifetime of the interface, nor does it address the role of surface defect sites.

For a semiconductor interface that fails the thermodynamic criteria, the Faradaic current is partitioned into the kinetic competition between the desired electrochemical fuel forming reaction and the undesirable surface degradation. For example, even for thermodynamically unstable photoanodes, if the solution electrochemical process sufficiently outpaces the surface decomposition redox process, the photoanode could have some useful 'metastability.'[5] The experimental elucidation of the specific kinetic metrics, which are given by the relevant rate constants of the competitive kinetic pathways, is rare. However, a recent report showing the unexpected long-lived stability of unprotected GaAs photocathodes in acid[6] is an example that illustrates that such kinetic information, rather than just Pourbaix diagrams and the thermodynamics of Fig. S4-1, is needed to understand and predict electrode longevity. With the use of the photoabsorber as the surface for the catalytic oxidation or reduction of water, conditions of extreme pH, either 0 or 14, are created, which can induce chemical corrosion of the semiconductor. This holds for catalytic structures deposited on the surface of the light absorber as well, whether they be interfacial or molecular in nature and they may not tolerate such pH conditions either. Stability under these extreme conditions produces severe constraints upon the search for suitable catalytic semiconductor interfaces. It is logical to seek systems that operate at a neutral pH; while few options have been reported in this regime,[7] the self-healing catalytic surfaces of Co and Ni oxides are proof that they do exist.[8]

One factor that can impact charge-transfer and corrosion/oxidation kinetics is the presence of surface states. Defined as under-coordinated surface atoms that possess active electronic states within the bandgap, surface states can strongly influence corrosion rates. In some cases, they can serve as initiation points for corrosion/oxidation. Developing functionalization strategies or designing targeted adsorbates specific to these sites could measurably and usefully slow chemical surface degradation. In the inhibition of electrochemical corrosion reactions by surface states, their trapping/detrapping can limit the steady-state accumulation of holes at a photoanode, resulting in this picture in a hole quasi-Fermi level being fixed above ${}_{p}\mathbf{E}_{decomposition}$. Determining whether this approach could be done specifically and intentionally without compromising the kinetics of the desired catalytic reactions requires further analysis.

Another facet of semiconductor photoelectrode operation worth consideration is self-passivation. Self-passivation is the formation of an insoluble product layer from the initial semiconductor dissolution/oxidation that can both negatively and positively impact photoelectrode operation. It is a layer that blocks solution access to the light absorbing semiconductor, but if it results in an electroactive stoichiometry that is stable, or a thin layer that allows tunneling of charge, the initial corrosion could be viewed as productive. With insight and control over surface dissolution such surface layers could even be designed by intent. However, if instead a highly disordered, low density layer that is thermodynamically unstable forms first, self-passivation may not be realized, as is the case with $BiVO_4$ where a chemically robust bismuth oxide surface layer is expected to develop.[4] As a counter example, experimental evidence supports the self-passivation of copper vanadates,[9] despite presumably similar degradation pathways that initially involve vanadium dissolution.

How stable is stable enough for an interface? One obvious criterion for stability is a lifetime sufficient for payback of the energy invested in making the semiconductor material itself, derived from the number of fuel

equivalents produced by the photoelectrode.[10] Of course, the actual and practical service lifetime must be many times greater than this payback lifetime for the semiconductor in order for the overall device to be cost-effective. In a technical sense, this also sets a lower limit for the lifetime of any surface electrocatalyst employed. Eventual corrosion threshold levels to be adopted in the quantification and categorization of semiconductor stability should be couched in terms of such energy payback times.

Advances in this control of kinetic processes will rely upon the most relevant and insightful experimental methods that can and should be employed to understand photoelectrode degradation mechanisms. These range from techniques present in the laboratories of most individual researchers to sophisticated measurements for specific photosystems, as might be found in the dedicated analytical facility discussed earlier, to beamline end station experimentation at large synchrotron facilities. Measurements from simple electroanalytical methods such as chronoamperometry and voltammetry are often made to ascertain susceptibility to photocorrosion/oxidation and to quantify failure. While useful, these data provide comparatively little insight on the underlying mechanisms of failure and/or surface change. Such information is not unattainable, though. For example, the dynamics of semiconductor dissolution in water has been studied in detail in noteworthy studies of Si/water interfaces by scanning probe methods.[11,12]

In recent years, an array of powerful *in situ* and *operando* characterization tools have been developed to offer new routes to overcoming knowledge gaps relating to material transformations in active environments. However, many of these methods have not been fully utilized to study semiconductor corrosion/oxidation processes. Significant opportunities do exist. For example, ambient pressure x-ray photoelectron spectroscopy now allows direct insight o solid/liquid interface, including chemical transformations of active electrodes and even the potential drop across the double layer.[13-15] X-ray absorption and emission spectroscopies,[16-18] x-ray microscopy[19], time resolved optical spectroscopies,[20,21] infrared spectroscopy,[22] and spectroscopic ellipsometry have further been developed to study semiconductor/solution interfaces under operation. Notable new methodologies for performing photoelectrochemistry within a transmission electron microscopy are being developed.[23-25] Through dedicated research in a variety of fields, the sophistication of these methods is continually improving and it is expected that they will play a critical role in the development of stable and efficient photoelectrochemical interfaces.

S4b Cooperativity in Interface Design

The harsh pH conditions of OER and HER can greatly perturb the energetics and structure of the semiconductor surface. In this case, the prototypical semiconductor band position diagrams[26] used to include or exclude semiconductors from either reduction or oxidation reactions based on the positions represented by Fig. S4-1 may then be misleading. A more cooperative view of the interfacial structure may be needed

In section **S3** above on novel semiconductors, a number of selection criteria were described. They included the thermodynamic energy offsets of the band positions vs. reactant redox energy, the kinetic overpotential of the

catalytic reaction, and the imperfect selectivity where the Faradaic efficiency less is than unity and the decomposition branching ratio favors decomposition. They all contribute to efficiency and stability of the overall system. These criteria can be addressed in a holistic, system-level perspective instead of dealing with these three as individual and mostly independent variables.

A consideration of the first criterion of thermodynamics deals with the light absorption, transport properties, and energetic positions of semiconductors and results in schemes to minimize such thermodynamic energy losses in a photoelectrode. For example, in the selection of a p-type semiconductor for photocatalytic proton reduction, the band level diagrams for various semiconductors are employed to choose from those where the conduction band energy is more negative than the potential of the normal hydrogen electrode (NHE).[2,26-2]As elaborated in the text, however, semiconductor band positions can vary from models at extreme pH and when modified with oxide or catalytic metal deposits. This will necessarily influence the kinetics at the interface.

Addressing the roles of the second and third criteria on catalytic overpotential and branching ratio selectivity at interfaces, the underlying material generally is not considered as part of the interfacial catalyst – typically the sub-surface and non-catalytically active surface layers are regarded as simply the source of electrons/holes with sufficient energy to carry out the reaction of interest. This perspective gives little weight to possible cooperative interactions with an underlying semiconductor or any oxide "passivation" interlayer to be found in the electrical/binding site environment, a lattice mismatch to generate strain in the catalyst or perhaps even in a density of states overlap with the catalyst. As a concept, adaptive and self-healing catalytic interfaces move away from this static model, although few examples are known.[34] The penetration of the active catalytic structural elements of the interface into the solid is an important theme in heterogeneous catalysts where the interaction of the active metal site with its underlying metal oxide support governs the kinetics. Catalytic interfaces are dynamic. For example, the metal Co and Ni oxides explored over past decades for water splitting appear not to be the active players. High resolution transmission electron microscopy show the oxides to have amorphous overlayers comprising metallate aggregates.[35-36] These molecular clusters comprising the amorphous oxide are indeed the active catalytic sites. The oxide serves to transport holes to the molecular active sites of the amorphous overlayer. Given this perspective on how the underlying semiconductor and/or metal oxide passivating layer can affect the catalytic overpotential and selectivity, including phases unintentionally generated at the semiconductor|catalyst interface, a broader view can be taken on the options in the design of PEC systems.

S4c Thin Layer Semiconductor Structures

The thin layer deposition technologies of the electronics and PV industries can be carried over into PEC design schemes. There are two characteristic forms of a junction buried beneath the PEC active surface , one being a traditional multilayer GaAs/$GaInP_2$ water splitting system from Turner[38] and another from Nocera where an amorphous Si/SiGe PV cell drives a self-repairing Co/Ni oxide layer for water splitting.[34,3 9]

Of more recent interest is the development of effective overlayer technology. Present ALD technology allows for an overlayer film on the semiconductor light absorber that minimizes defects at the nanometer level. [39-42]It is compatible with high-volume manufacturing of thin film structures[43] with both high-pressure and reel-to-reel ALD toolsets having been demonstrated[44] suggesting its potential for application at scale. These attributes of ALD make it possible to avoid the use of thick protective overlayers which contribute to greater parasitic light absorption and reflection losses and limit the effective electrode conductance and the photovoltage of simple Schottky photodiode-type cells. They also make ALD attractive for deposition of pinhole-free thin film coatings of thermodynamically stable materials on high quality semiconductor light absorbers such as silicon or gallium arsenide.

Fig. S4-2 illustrates several designs for the thin layer structures which are possible with these characteristics of overlayers. Alternative forms of photoelectrode protection include variable thickness transparent conducting oxide-like coatings with appropriate work function to achieve large photovoltage and required thermodynamic stability against corrosion. Very thin layers of more electronically insulating coatings with low series resistance can be deposited with a high charge storage capacity. p^+n or n^+p buried junctions fabricated in the absorber are also able to decouple band bending in the semiconductor from charge transfer across the coating.[45]

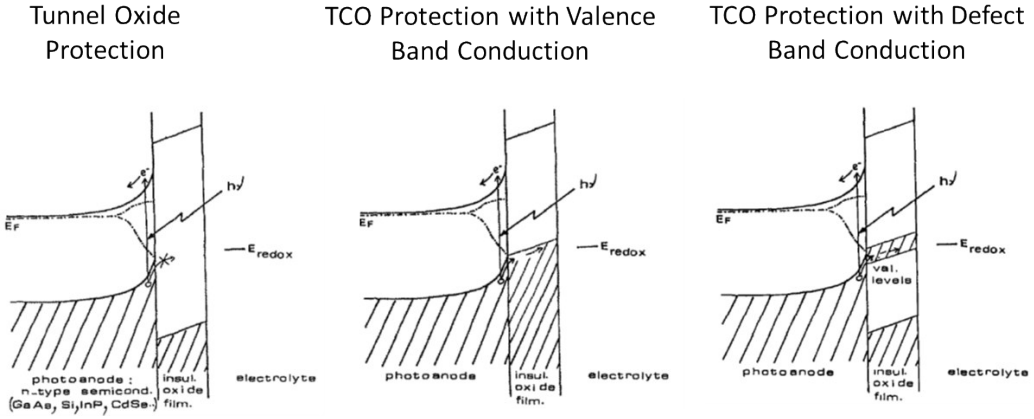

Fig. S4-2 Alternatives for photoanode protection. Before ALD, tunnel oxide protection of efficient photoanodes was thought to be impossible because thick layers were required for corrosion protection, giving unacceptably high electrical resistance. (From Ref. 46 with permission. Copyright 1989 Elsevier.)

ALD-TiO_2 coatings have proven very useful in corrosion suppression at silicon photoelectrodes.[47] Post deposition annealing of the films at 450°C and 900°deposition greatly enhances film stability and is consistent with densification and crystallization of the films, which are initially amorphous and relatively hydrated as a result of the ALD reaction conditions and precursor chemistry, as has been discussed in detail in prior.[48] Iridium can be evaporated on the TiO_2 as a catalytic layer for oxygen evolution; initial results obtained from ultrathin IrO_x-TiO_2 alloy thin films on silicon photoanodes using "super-cycle" ALD suggest that post-deposition annealing, resulting in partial crystallization, also produces enhanced stability with respect to IrO_x dissolution at water oxidation potentials in concentrated acid and base.[49] Similar results have been observed at CoOx interfaces.[50]

With the use of evaporated Ir as an OER catalyst in these experiments, the surface of the Ir oxidizes readily during water oxidation, producing an IrO_x layer in contact with the electrolyte. This places the catalyst film in a state of biaxial compression as a result of the volume expansion associated with Ir oxidation and the elastic constraint provided by bonding of the Ir to the underlying TiO_2 layer, which creates its own susceptibility to degradation. However, without the TiO_2 layer in the anode structure, the Ir OER catalyst debonds readily from an underlying SiO_2 layer on the silicon substrate, often exposing the entire tested area.[39] While ALD of such oxide layers may have reduced the instabilities from overlayer delamination, it has emphasized catalyst adhesion as a failure mechanism.[51]

References.

1. H. Gerischer, *J. Electroanal. Chem. Interfacial Electrochem.,* 1977, **82**, 133−143.
2. S. Chen and L.-W. Wang, *Chem. Mater., 2012,* **24**, 3659-3666.
3. T.W. Hamann *Dalton Trans.*, 2012, **41**, 7830-7834.
4. F. M. Toma, J. K. Cooper, V. Kunzelmann, M. T. McDowell, J. Yu, D. M. Larson, et al., *Nature Commun., 2016,* **7**, 12012.
5. X. Zhou, R. Liu, K. Sun, Y. Chen, E. Verlage, S. A. Francis, et al., *ACS Energy Letters, 2016*, **1**, 764-770.
6. J. L. Young, K. X. Steirer, M. J. Dzara, J. A. Turner and T. G. Deutsch, *J. Mater. Chem. A*, 2016, **4**, 2831-2836.
7. J. Jin, K. Walczak, M. R. Singh, C. Karp, N. S. Lewis and C. Xiang, *Energy Environ. Sci.*, 2014, **7**, 3371-3380.
8. Y. Surendranath, M. W. Kanan and D. G. Nocera, *J. Am. Chem. Soc.*, 2010, **132**, 16501–16509.
9. L. Zhou, Q. Yan, J. Yu, R. J. R. Jones, N. Becerra-Stasiewicz, S. K. Suram et al., *PCCP,* 2016*,* **18**, 9349-9352.
10. P. Zhai, S. Haussener, J. Ager, R. Sathre, K. Walczak, K. J. Greenblatt and T. McKone, *Energy Environ. Sci.,* 2013, **6**, 2380-2389.
11. M. A. Hines, *Int. Rev. Phys. Chem*, **2001**, *20*, 645-672.
12. P. Allongue, V. Kieling and H. Gerischer, *Electrochim. Acta.,* **1995**, *40*, 1353-1360.
13. M. Favaro, B. Jeong, P. N. Ross, J. Yano, Z. Hussain, Z. Liu and E. J. Crumlin, *Nature Commun.,* 2016. **7**, 12695.
14. M. F. Lichterman, S. Hu, M. H. Richter, E. J. Crumlin, S. Axnanda, M. Favaro, et al., *Energy Env. Sci.*, 2015, **8**, 2409-2416.
15. M. Favaro, R. Uecker, S. Nappini, I. Píš, E. Magnano, H. Bluhm, et al., *J. Am. Chem. Soc., 2017,* **139**, 8960-8970.
16. D. Friebel, V. Viswanathan, D. J. Miller, T. Anniyev, H. Ogasawara, A. H. Larsen, C. P. O. Grady, J. K. Narskov, and A. Nilsson, *J. Am. Chem. Soc.*, 2012, **134**, 9664.
17. D. Friebel, M. Bajdich, B S. Yeo, M. W. Louie, D. J. Miller, H. Sanchez Casalongue, et al., *PCCP, 2013,* **15**, 17640-17643.
18. M. Farmand, A. T. Landers, J. C. Lin, J. T. Feaster, J. W. Beeman, Y. Ye, et al., PCCP, 2019, **21**, 5402-5408.
19. J. Lim, Y. Li, D. H. Alsem, H. So, S. C. Lee, P. Bai, et al., *Science* **353**, 2016, 566-571.
20. Y. Yang, J. Gu, J. L. Young, E. M. Miller, J. A. Turner, N. R. Neale and M. C. Beard, *Science,* **350**, 2015, 1061-1065.
21. M. Barroso, C. A. Mesa, S. R. Pendlebury, A J. Cowan, T. Hisatomi, K. Sivula, M. Grätzel, D. R. Klug and James R. Durrant, *PNAS, 2012,* **109**, 15640-15645.
22. N. J. Firet and W. A. Smith, *ACS Catalysis* **7**, 606 (2017-612.
23. B. Xiang., D. J. Hwang, J. Bin In, S. G. Ryu,, J. H. Yoo, O. Dubon, A. M. Minor and C. P. Grigoropoulos, *Nano Lett*., 2012, 12, 2524–2529.
24. F. Cavalca, A. B. Laursen, B. E. Kardynal, R. E. Dunin-Borkowski, S. Dahl, J. B. Wagner and T. W. Hansen, *Nanotechnology*, 2012, **23**, 075705.

25. B. K. Miller and P. A. Crozier, *Microsco, and Microanal.*, 2013, **19**, 461–469.
26. M. Gratzel, M., *Nature,* 2001, **414**, 338-344.
27. A. J. Nozik and R. Memming J. Phys. Chem. 1996, **100**, 13061-13078.
28. R. van de Krol and M. Grätzel, *Photoelectrochemical Hydrogen Production*, Springer, Boston, MA, 2012.
29. D. Bae, B. Seger, P. C. K. Vesborg, O. Hansen and Ib Chorkendorff, *Chem. Soc. Rev.,* 2017, **46**, 1933-1954.
30. H Gerischer, *J. Electroanal. Chem.*, 1983, **150**, 553-569.
31. A.J. Nozik, *Ann. Rev. Phys. Chem.* 1978, **29**, 189-222.
32. G. A. Parks, *Chem. Rev.*, 1965, **65**, 177–198.
33. N. C. Anderson, G. M. Carroll, R. T. Pekarek, S. T. Christensen, J. van de Lagemaat and N. R. Neale, *J. Phys. Chem. Lett.*, 2017, **8**, 5253-5258.
34. S.Y. Reece, J. A. Hamel, K. Sung, T. D. Jarvi, A. J. Esswein, J. J. H. Pijpers, D. G. Nocera, *Science*, 2011, **334**, 645–648.
35. A. Bergmann, E. Martinez-Moreno, D. Teschner, P. Chernev, M. Gliech, J. Ferreira de Araujo, et al., *Nat. Commun.*, 2015, **6,** 1-9.
36. D. Gonzalez-Glores, I. Sanchez, I. Zaharieva, K. Klingan, J. Heidkamp, P. Chernev, et al., *Angew. Chem. Int. Ed.*, 2015, **54**, 2472-2476.
37. A. C Nielander, M. R. Shaner, K. M. Papadantonakis, S. A. Francis and N. S. Lewis, Ener. Env. Sci. 2015, **8**, 16-25.
38. O. Khaselev and J. A. Turner, *Science*, 1998, **280**, 425-427.
39. Y. W. Chen, J. D. Prange, S. Duhnen, Y. Park, M. Gunji, C. E. D. Chidsey, and P. C. McIntyre, *Nat. Mater.*, 2011, **10**, 539−544.
40. B. Seger, D. S. Tilley, T. Pedersen, P. C. K. Vesborg, O. Hansen, M. Gratzel, and I. Chorkendorff, *RSC Adv*., 2013, **3**, 25902−25907.
41. S. Hu, M. R. Shaner, J. A. Beardslee, M. Lichterman, B. S. Brunschwig, and N. S. Lewis, *Science,* 2014, **344**, 1005−1009.
42. S. M. George, *Chem. Rev.,* 2010, **110**, 111−131.
43. A. Foroughi-Abari and K. Cadien, *Atomic Layer Deposition for Nanotechnology, in Nanofabrication,* 2012, Springer. pp. 143-161.
44. W. M. M. Kessels and M. Putkonen, *MRS Bull.,* 2011, **36**, 907-913.
45. A. G. Scheuermann, J. P. Lawrence, K. W. Kemp, T. Ito, A. Walsh, C. E. D. Chidsey, P. K. Hurley and P. C. McIntyre, *Nat. Mater.*, 2016, **15**, 99-105.
46. G. Campet, C. Puprichitkun and Z. W. Sun, *J. Electroanal. Chem. Interfacial Electrochem.,* 1989, **269**, 435−445.
47. G. C. Correa, B. Bao and N. C. Strandwitz, *ACS Appl. Mater. Interfaces*, 2015, **7**, 14816−14821.
48. G. I. Kelsall and D. J. Robbins, *J. Electroanal. Chem.,* 1990, **283**, 135-157.
49. O. L. Hendricks, P. C. McIntyre and C. E. D. Chidsey, *Chem. Mater.,* 2019, **31**, 90-100.
50. J. Yang, J. K. Cooper, F. M. Toma, K. A. Walczak, M. Favaro, J. W. Beeman, et al., *Nat. Mater.*, 2017, **16**, 335–341.
51. R. Tang-Kong, R. Winter, R. Brock, J.Tracy, M. Eizenberg, R. H. Dauskardt and P. C. McIntyre, *J.Electrochem.Soc.* 2018, **165**, H1072-1079.